Evaluating Uncertainty in Aerosol Forcing of Tropical Precipitation Shifts

Amy H. Peace[1,4], Ben B. B. Booth[2], Leighton A. Regayre[1], Ken S. Carslaw[1], David M. H. Sexton[2], Céline J. W. Bonfils[3], John W. Rostron[2]

[1]Institute for Climate and Atmospheric Science, University of Leeds, Leeds, UK
[2]Met Office Hadley Centre, Exeter, UK
[3]Lawrence Livermore National Laboratory, Livermore, CA, USA
[4]College of Engineering, Maths and Physical Science, University of Exeter, Exeter, UK

Correspondence to: Amy H. Peace (A.H.Peace@exeter.ac.uk)

Please ignore track changes to references – these are due to opening document on new laptop with updated Mendeley version. Line numbers in reply refer to the pdf without tracked changes.

Abstract. An observed southward shift in tropical rainfall over land between 1950 and 1985, followed by a weaker recovery post 1985, has been attributed to anthropogenic aerosol radiative forcing and cooling of the Northern Hemisphere relative to the Southern Hemisphere. We might therefore expect models that have a strong historic hemispheric contrast in aerosol forcing to simulate a further northward tropical rainfall shift in the near-term future when anthropogenic aerosol emission reductions will predominantly warm the Northern Hemisphere. We investigate this paradigm using a perturbed parameter ensemble (PPE) of transient coupled ocean-atmosphere climate simulations that span a range of aerosol radiative forcing comparable to multi-model studies. In the 20th century, in our single-model ensemble, we find no relationship between the magnitude of pre-industrial to 1975 inter-hemispheric anthropogenic aerosol radiative forcing and tropical precipitation shifts. Instead, tropical precipitation shifts are associated with major volcanic eruptions and are strongly affected by internal variability. However, we do find a relationship between the magnitude of pre-industrial to 2005 inter-hemispheric anthropogenic aerosol radiative forcing and future tropical precipitation shifts over 2006 to 2060 under scenario RCP8.5. Our results suggest that projections of tropical precipitation shifts will be improved by reducing aerosol radiative forcing uncertainty, but predictive gains may be offset by temporary shifts in tropical precipitation caused by future major volcanic eruptions.

1 Introduction

The interaction of atmospheric aerosols with clouds and radiation is the largest cause of uncertainty in the radiative forcing of the Earth system over the industrial period (e.g. (Bellouin et al., 2020; Myhre et al., 2013)). Atmospheric aerosols have short residence times of days to weeks, therefore the strongest radiative effects of aerosols occur relatively close to emission sources. The increase in anthropogenic aerosol emissions over the industrial era has therefore caused a negative radiative forcing mainly in the Northern Hemisphere. This hemispheric nature of anthropogenic aerosol radiative forcing has been linked to observed

35 shifts in tropical precipitation and understood using idealised and transient climate model simulations (Allen et al., 2015; Hwang et al., 2013; Williams et al., 2001; Rotstayn and Lohmann, 2002; Rotstayn et al., 2000; Chang et al., 2011; Evans et al., 2020; Chemke and Dagan, 2018; Bonfils et al., 2020). Most notably, anthropogenic aerosol emissions that increased rapidly across Europe and North America up to the 1980s (Lamarque et al., 2010) have been linked to an observed southward shift in tropical precipitation, which was associated with widespread drying of the Sahel between the 1950s and 1980s (Biasutti and

40 Giannini, 2006; Allen et al., 2015; Kang et al., 2021; Herman et al., 2020; Ackerley et al., 2011; Booth et al., 2012; Dong et al., 2014; Hirasawa et al., 2020). Over recent decades there has been a partial northward return of tropical precipitation alongside a modest recovery of rainfall over the Sahel (Giannini and Kaplan, 2019) and India, but increased drought in the Northeast Brazilian region (Utida et al., 2019). Natural aerosols from major volcanic eruptions can also cause a negative radiative forcing primarily in one hemisphere, dependent on the latitude of the eruption (Haywood et al., 2013).

45 Latitudinal shifts of tropical precipitation are intertwined with perturbations to the Hadley Circulation and movement of the Intertropical Convergence Zone (ITCZ). The theoretical energetic framework links the position of the ITCZ to the interhemispheric energy balance. As such, a perturbation to the inter-hemispheric energy balance, particularly in the extra tropics, can trigger a shift in the position of the ITCZ and associated tropical precipitation (Kang et al., 2008, 2009, 2018a). From an atmospheric perspective, the Hadley Cell would adjust to transport more energy northwards in response to the anomalous inter-

50 hemispheric energy balance imposed by a cooling of the Northern Hemisphere, for example, by anthropogenic aerosol forcing (Hwang et al., 2013). From the perspective of a dynamical ocean, wind-driven shallow overturning cells also act to transport energy in the same direction as the atmosphere (Green and Marshall, 2017; Kang, 2020). Hence, in a framework where a dynamical ocean is taken into account, the atmospheric response of the ITCZ to an inter-hemispheric energy imbalance is partially dampened. In addition to aerosol radiative forcing, other forcing agents such as changes in high-latitude ice cover and

55 ocean circulation can alter the inter-hemispheric energy balance (Chiang and Bitz, 2005; Chiang and Friedman, 2012; Broccoli et al., 2006). Migrations in tropical precipitation over the 20th century have also been linked to variability in the difference in sea surface temperature between the Northern and Southern Hemispheres (Chiang and Friedman, 2012; Thompson et al., 2010). Because there are multiple drivers, there remains debate over whether the shifts in tropical precipitation observed over the 20th century can be attributed to anthropogenic aerosols, other forced responses, natural climate variability, or a

60 combination of these.

Anthropogenic aerosol emissions are projected to decline in the future in response to increasingly stringent air quality and climate change mitigation policies (Rao et al., 2017; van Vuuren et al., 2011b). Reductions in anthropogenic aerosol emissions will lead to a warming of climate relative to present day that will primarily affect the Northern Hemisphere, and could lead to a northward shift in tropical precipitation (Allen, 2015; Rotstayn et al., 2015). However, identifying the drivers of future

65 tropical precipitation shifts is complex for a number of reasons. Warming of Northern Hemisphere landmasses caused by greenhouse gases could too lead to a northward shift in tropical precipitation (Frierson and Hwang, 2012; Friedman et al., 2013). If so, the relative warming from anthropogenic aerosol reductions and warming from increasing greenhouse gases could have an additive effect on any northward tropical precipitation shift, rather than acting in opposing directions as seen over the

90   20th century, making attribution to a particular forcing agent even harder to disentangle (Friedman et al., 2013). Throughout
the 21st century, the climate response to warming also adds a layer of complexity to the attribution of tropical precipitation
changes. Climate feedbacks, such as sea-ice feedbacks or changes in Atlantic Meridional Overturning Circulation (AMOC)
strength can modulate the position of the ITCZ, leading to a tug-of-war between different forcing and feedback components
(McFarlane and Frierson, 2017; Mamalakis et al., 2021). Changes in large-scale circulation associated with warming (e.g. wet-

95   gets-wetter paradigm) can also affect the tropical precipitation distribution and could mask an identifiable signal for latitudinal
tropical precipitation shifts (Friedman et al., 2013).

Large uncertainty in anthropogenic aerosol radiative forcing limits our understanding of historical changes in climate and the
drivers of tropical precipitation and ITCZ migrations. Multi-model studies show the strength of the hemispheric difference in
aerosol radiative forcing correlates with the magnitude of tropical precipitation shifts in the 20th century. Coupled Model Inter-

100   comparison Project 5 (CMIP5) models with relatively detailed representations of aerosol-cloud interactions simulate a further
southward migration of tropical precipitation over 1950 to 1985 (Allen et al., 2015) and better reproduce decadal drivers of
Indian rainfall (Choudhury et al., 2021). However, multi-model ensembles (MMEs) represent a collection of models which
vary not only in how they represent physical processes, but in the complexity and range of processes that they represent at all.
As such, it is hard to interpret differences across multi-model ensembles and link them back to processes. Whether or not

105   aerosol reductions will be a main driver of tropical precipitation shifts in the future remains unclear, yet it is likely the large
uncertainty in aerosol forcing will cause uncertainty in projected tropical precipitation shifts (Byrne et al., 2018a).

The influence of aerosol radiative forcing on tropical precipitation shifts has not previously been investigated using perturbed
parameter ensemble (PPEs). PPEs explore model uncertainties by perturbing influential uncertain model parameters within
their plausible ranges. An advantage of using PPEs is that differences in climate response across the ensemble can often be

110   linked back to known differences in the perturbed parameters – which can yield new insights into what causes spread in climate
model response. Here, we make use of a PPE of the coupled ocean-atmosphere model HadGEM3-GC3.05 that was developed
for UK National Climate Projections (UKCP18). In the PPE, 47 parameters are perturbed across a range of model schemes.
The perturbed parameters resulted in an emergence of a wide range of aerosol forcings across the PPE, but a relatively smaller
range of climate sensitivities, as shown in Figure 1. In principle, the PPE may therefore be a useful tool to assess the relationship

115   between anthropogenic aerosol radiative forcing uncertainty and tropical precipitation shifts over the 20th and 21st centuries.

2 Methods

2.1 Perturbed Parameter Ensemble of HadGEM3-GC3.05

This study utilises a perturbed parameter ensemble (PPE) of climate model simulations that was designed to inform UK Climate Projections 2018 (UKCP18). One of the key aims of UKCP18 was to provide a flexible data set with a small sample size to support a wide range of impact assessments (Sexton et al., 2021). The design of the PPE was therefore focused on providing a small number of transient coupled-ocean atmosphere simulations that sample plausible and diverse climate changes for a given emissions scenario (Murphy et al., 2018; Yamazaki et al., 2021). The resulting PPE spans a large fraction of the AR6 very likely range of aerosol ERF, but a smaller range of climate sensitivity (Figure 1). Similar to multi-model ensembles, the PPE therefore provides an opportunity to investigate the role of aerosol forcing uncertainty on tropical precipitation shifts in an 'ensemble of opportunity', but with the advantage that differences in climate responses can be linked back to underlying parameters/processes. Below we summarise the design of this PPE and how we utilise 13 PPE members to explore the relationship between aerosol radiative forcing uncertainty and tropical precipitation shifts.

Comparison of aerosol ERF and climate sensitivity in the PPE

(a)

(b)
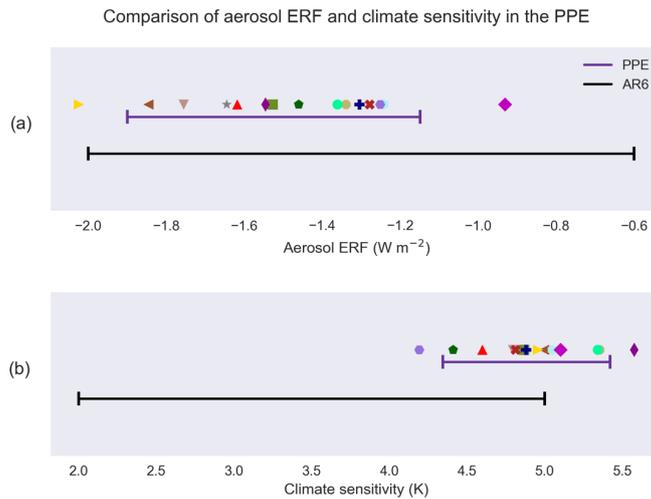
Figure 1: Range of aerosol ERF (a) and equilibrium climate sensitivity (b) across the PPE and AR6. The PPE error bars shows the 90% range across 15 PPE members compared with the AR6 90% 'very likely' ranges from (Forster et al., 2021)**. We use 13 PPE members in this study, excluding two shown in this figure due to model drifts.**

The base model used in this work is version 3.05 of the UK Hadley Centre Unified Model (HadGEM3-GC3.05), which is a global coupled ocean-atmosphere model. HadGEM3-GC3.05 includes many of the main improvements that were made to GC3.0 to create GC3.1 that was submitted to CMIP6 (Williams et al., 2018; Walters et al., 2019). The atmospheric component is HadGEM3-GA7.05 (Williams et al., 2018). The atmospheric and land components are configured at 'N216' resolution (approximately 60 km horizontal spacing of grid boxes at mid-latitudes), with 85 vertical atmospheric levels. HadGEM3-GC3.05 incorporates the modal version of the GLObal Version of Aerosol Processes (GLOMAP-mode) which simulates new particle formation, gas-to-gas particle transfer, aerosol coagulation, cloud processing of aerosol and aerosol deposition of sulphate, sea salt, dust, black carbon and particulate organic species (Mann et al., 2010). The ocean and sea-ice model components are NEMO and CICE respectively (Hewitt et al., 2011). The ocean component is eddy permitting with a resolution of ¼° and finer. Ocean components of Global Climate Models (GCMs) that are higher resolution and resolve eddies (such as this model version) can affect the mean state of the ocean, climate variability and climate response, in comparison to lower resolution ocean components (Hewitt et al., 2020).

Experts selected 47 model parameters from the physical atmosphere, aerosol and land surface model components of HadGEM3-GC3.05 to perturb across their uncertain ranges in order to sample the parametric model uncertainty in climate projections. The 47 model parameters chosen to be perturbed are from the model schemes representing convection, boundary layer, gravity wave drag, cloud radiative and microphysical properties, aerosol and land surface properties. A description of perturbed parameters is given in Table S1, and the selection process for these model schemes and parameters is described in further detail in Sexton et al., 2021.

Each model simulation in a PPE framework consists of a unique combination of perturbed model parameter values. We refer to each unique combination of parameter values as a 'model variant'. Current computational constraints meant that a total of 25 transient coupled ocean-atmosphere simulations could be produced for UKCP18. These 25 model variants were required to sample the uncertainty across the 47 perturbed parameters, whilst remaining plausible when evaluated against observed climate variables and representing diversity in climate responses. Therefore, multi-stage filtering of an initial large sample of model variants was undertaken for UKCP18 to identify a plausible and diverse subset to be used in the transient simulations. We briefly summarise the stages of the filtering process below aided by Figure 2 and direct the reader to the literature (Sexton et al., 2021; Yamazaki et al., 2021) where the process is described in full for further information.

Deleted: (Williams et al., 2018; Walters et al., 2019)

Deleted: (Williams et al., 2018)

Deleted: (Mann et al., 2010)

Deleted: (Hewitt et al., 2011)

Deleted: (Hewitt et al., 2020)

Deleted: ¶

Formatted: Level 2, Space Before: 12 pt, After: 12 pt, Keep with next

Deleted: A perturbed parameter ensemble of the above model set up was designed for UK Climate Projections 2018 (UKCP18) to sample the uncertainty in future climate changes for a given emission scenarios (Murphy et al., 2018; Yamazaki et al., 2021). This PPE samples the uncertainty in

Deleted: (Sexton et al., 2021)

Figure 2: Schematic showing the stages in the design process used in UKCP18 to provide a small subset of model variants that sample a diverse climate response and are plausible when evaluated against historical climate. In this study, we use 13 PPE members of the aerosol ERF and transient coupled ocean-atmosphere experiments which are highlighted in the purple boxes.

Initially, 2800 model parameter combinations were created that sample the uncertainty across the 47 perturbed parameters. Latin Hypercube sampling was used to select the initial wave of parameter combinations. The Latin Hypercube sampling approach maximises the minimum distance between points to ensure good coverage of the multi-dimensional 'parameter space' created by simultaneously perturbing 47 model parameters. After the model variants were created, the filtering process first involved assessing the performance of model variants against observed climate variables using cheaper atmosphere-only experiments. The performance of the initial 2800 model variants was assessed using five-day weather hind-casts (start dates covering 2008 to 2009). A remaining 557 model variants were then assessed for performance using five-year (2005 to 2009)

atmosphere-only simulations. This filtering process left 39 remaining model variants considered plausible. These 39 model variants were reduced to a 25-member PPE of diverse members that would sample a broad range of climate responses. Three idealized atmosphere-only experiments that are similar to those used in CMIP5 (Taylor et al., 2012) were used to assess the diversity in climate response across the model variants: aerosol effective radiative forcing (ERF) between 1860 and 2005, ERF due to a quadrupling of CO_2, and sea surface temperature (SSTs) patterns prescribed for a global warming of 4 °C. Diversity was assessed using a combination of metrics from these idealized experiments, and transient coupled ocean-atmosphere simulations were created for the 25 most diverse, plausible model variants. The filtering process to identify the 25 model variants is described in further detail in Sexton et al., 2021. Lastly, the transient PPE simulations were filtered based on their performance over 1900 to 2005, as described in Yamazaki et al., 2021. This multi-stage process left 15 (out of an initial 2800) remaining model variants that sample known model uncertainties and hence provide, for a given emissions scenario, a range of climate responses. The aerosol ERF experiment that was used in the diversity filtering stage shows that these 15 model variants span a large range of aerosol ERF, as shown in Figure 1. However, additional idealised 4 x CO_2 coupled-ocean atmosphere simulations that were created following the completion of UKCP18 to diagnose ECS for the PPE (Sexton et al., 2020), show that the 15 model variants sample a comparatively smaller range of climate sensitivity. We use 13 of the 15 remaining ensemble members in this study, excluding a further two members on the basis that these members show steady weakening of the AMOC (Sexton et al., 2020).

Historical emissions were prescribed in the ensemble members up to 2005, then forking into the Representative Concentration Pathway (RCP) scenarios RCP8.5 and RCP2.6 to 2100. The RCPs provide a range of greenhouse gas (GHG) concentrations and emission pathways that span a range of total radiative forcing at 2100. RCP8.5 is a high emissions scenario, with GHG emissions assumed to rise substantially out to 2100 (Riahi et al., 2011). In contrast, RCP2.6 assumes aggressive measures to substantially reduce future GHG emissions (van Vuuren et al., 2011a). The RCP scenarios assume successful implementation of air quality legislation, but RCP2.6 has approximately double the reduction of air pollutant emissions by 2030 compared to RCP8.5 (Riahi et al., 2011).

In addition to model uncertainty that can be sampled using PPEs or MMEs, uncertainty in climate projections can arise from scenario uncertainty and internal variability. We use the small 4-member initial condition ensembles of HadGEM3-GC3.1-LL and HadGEM-GC3.1-MM that were submitted to CMIP6 (Andrews et al., 2020) to provide an idea of how internal variability alone can generate uncertainty in climate responses for a similar model version. The HadGEM-GC3.1-MM ensemble is the same resolution as the PPE, whereas the HadGEM-GC3.1-LL ensemble is lower resolution ('N96'; approximately 135 km horizontal spacing of grid boxes at mid-latitudes).

2.2 Quantifying Shifts in Tropical Precipitation

We use the 13 transient coupled ocean-atmosphere simulations described above to quantify shifts in tropical precipitation over the 20th and 21st centuries. We define the latitudinal position of the ITCZ and tropical precipitation, Φ_{ITCZ} (degrees), as the median of annual mean precipitation (mm day^{-1}) over area-weighted regional means between 20 °S and 20 °N. Several studies

have used this definition to quantify changes in the position of the ITCZ and tropical precipitation (Frierson and Hwang, 2012; Donohoe et al., 2013; Atwood et al., 2020; Evans et al., 2020; Moreno-Chamarro et al., 2020; Green et al., 2017; Green and Marshall, 2017). We calculate the linear trend of the 5-year rolling mean value of Φ_{ITCZ} over multi-decadal periods in the 20th and 21st centuries over three regions – Global, Atlantic and Pacific, where the Atlantic is defined as 75 °W to 30 °E, and the Pacific as 150 °E to 75 °W.

2.3 Inter-Hemispheric Temperature and Radiative Forcing

To study the drivers of the ITCZ shifts across the PPE, we calculate the Spearman's rank correlation coefficient of the decadal trend in Φ_{ITCZ} with variables related to the inter-hemispheric energy balance. These variables include the trend in the inter-hemispheric difference in surface air temperature and implied total radiative forcing, plus the inter-hemispheric difference in historical anthropogenic aerosol ERF. We also evaluate the role of cloud and non-cloud shortwave radiative responses, as well as the role of aerosol optical depth (AOD).

The inter-hemispheric difference is calculated as the difference between area-weighted Northern Hemisphere (0 °N to 60 °N) and Southern Hemisphere (0 °S to 60 °S) means and referred to as 'inter-hemispheric' herein. The inter-hemispheric variables are calculated over both land and ocean, unless specified. Linear trends of the inter-hemispheric variables are calculated from a 5-year rolling mean.

The implied total radiative forcing for the transient PPE was estimated at each grid box using the formula derived from (Gregory and Forster, 2008):

$$(1) \quad \Delta F_{Im} = \Delta F_{TOA} - \lambda \Delta T$$

where ΔF_{Im} is the implied radiative forcing of interest, ΔF_{TOA} is the change in annual mean net top of atmosphere flux relative to a reference period, ΔT is the change in global annual mean surface air temperature relative to a reference period, and λ is the climate feedback parameter. In this convention, positive feedback components are represented by a positive contribution to λ. In the PPE case, the value for λ was estimated using the approach in Gregory and Forster (2008), where for an abrupt 4 x CO_2 experiment, λ is the regression slope between radiative forcing and global temperature change, taking account of model drifts in the control runs (Sexton et al., 2020). In the case of the small HadGEM3-GC3.1 initial condition ensembles, we estimate ΔF_{Im} using a 1850 to 1870 reference period and a feedback parameter value of -0.86 W m^{-2} K^{-1} (following (Andrews et al., 2019).

For PPE members, shortwave cloud and non-cloud radiative responses were estimated using the approximate partial radiative perturbation (APRP) method (Taylor et al., 2007). The APRP method uses a single-layer radiative transfer model to decompose climate model output into three components: the change in shortwave radiation due to cloud, the change in shortwave radiation due to non-cloud atmospheric scattering and absorption, and the change in shortwave radiation due to surface albedo. Under this method, changes in the cloud component are solely due to changes in cloud properties, whereas changes in the non-cloud component are due to changes in aerosols, ozone and water vapour (Zelinka et al., 2014).

345 The idealized simulations that were used to assess the diversity of PPE members (Section 2.1), provide estimates of anthropogenic aerosol ERF at 2005 relative to 1860 for each PPE member in the transient coupled ocean-atmosphere simulations that we use to analyse tropical precipitation shifts. To better align with the historical time period analysed in this study, we completed additional simulations to provide estimates of anthropogenic aerosol ERF at 1975 relative to 1860 for our 13 PPE members. ERF was quantified as the change in radiative fluxes caused by changes in anthropogenic aerosol emissions

350 between 1860 and the industrial time period (1975 or 2005), with SSTs, sea-ice extent and greenhouse gas concentrations held constant at 2005 to 2009 values (rather than pre-industrial values as in CMIP studies; (Taylor et al., 2012)). Aerosol and physical atmosphere parameters are both important sources of uncertainty in aerosol ERF (Regayre et al., 2018). In our PPE, a total of 8 aerosol emission and process parameters are pertuned in combination with multiple physical atmosphere parameters that, amongst other responses, affect aerosol forcing. Our 13 ensemble members span a range of global mean 1860

355 to 2005 aerosol ERF of -2.0 to -0.9 W m^{-2}, which is larger and more negative, than the spread in 1850 to 2014 aerosol radiative forcing across 17 CMIP6 models (-1.37 to −0.63 W m^{-2}) (Smith et al., 2020), and similar to the estimated 1750 to 2014 aerosol ERF range from AR6 (−2.0 to −0.6 W m^{-2}; medium confidence) (Forster et al., 2021).

We use the inter-hemispheric 1860 to 1975 aerosol ERF when analysing tropical precipitation shifts in the 20th century, and the inter-hemispheric 1860 to 2005 aerosol ERF when analysing the 21st century. Aerosol ERF values are shown in Figure

360 S1-2. We do not have simulations from which to quantify the aerosol ERF in the near-term future. Hence, our analyses rely on the assumption that ensemble members with strong or weak near-present day aerosol radiative forcing will also have a strong or weak response to changes in aerosol emissions over the near-term future time periods as anthropogenic aerosol emissions decline.

3. Results and Discussion

365 ### 3.1 Tropical Precipitation Shifts over the 20th Century

We begin by examining the latitudinal shift of tropical precipitation (Φ_{ITCZ}) over the 20th century in our PPE. Figure 3 shows the 5-year rolling mean evolution of Φ_{ITCZ} over the historical period in the global, Atlantic and Pacific regional means. The PPE mean Φ_{ITCZ} migrates southwards over the 1940 to 1985 period (around 0.01 °latitude year^{-1} globally). This southward migration of tropical precipitation agrees with multi-model studies (CMIP3, CMIP5) and observations of tropical precipitation

370 over land that show tropical precipitation shifted southward in the second half of the 20th century (Hwang et al., 2013; Allen et al., 2015; Chung and Soden, 2017; Bonfils et al., 2020).

There are brief shifts in Φ_{ITCZ} in the years following major volcanic eruptions in the 20th century. The Φ_{ITCZ} time series without the 5-year smoothing applied is shown in Figure S3 to more precisely illustrate this effect. There is a northward shift in Φ_{ITCZ} following the Southern Hemisphere eruption of Mt Agung in 1963 and a southward shift following the Northern Hemisphere

375 eruption of El Chichón in 1982. Hence, our ensemble mean time series of Φ_{ITCZ} agrees with the literature (Haywood et al., 2013; Iles et al., 2013; Bonfils et al., 2020; Colose et al., 2016) showing the position of the ITCZ and tropical precipitation

responds to volcanic eruptions and shifts away from the hemisphere with the maximum stratospheric aerosol loadings. After 1985 (the period after which pollution controls are enforced in Europe and North America), there is a northward migration of Φ_{ITCZ} to the end of the 20th century. In the time series, individual members display greater inter-annual variability in the Pacific than in the Atlantic region. This could be due to different sequences of internal variability and/or different spatial-temporal evolution of the forced signal in the Atlantic and Pacific regions (e.g. (Diao et al., 2021)).

400

(a)

(b)

(c)
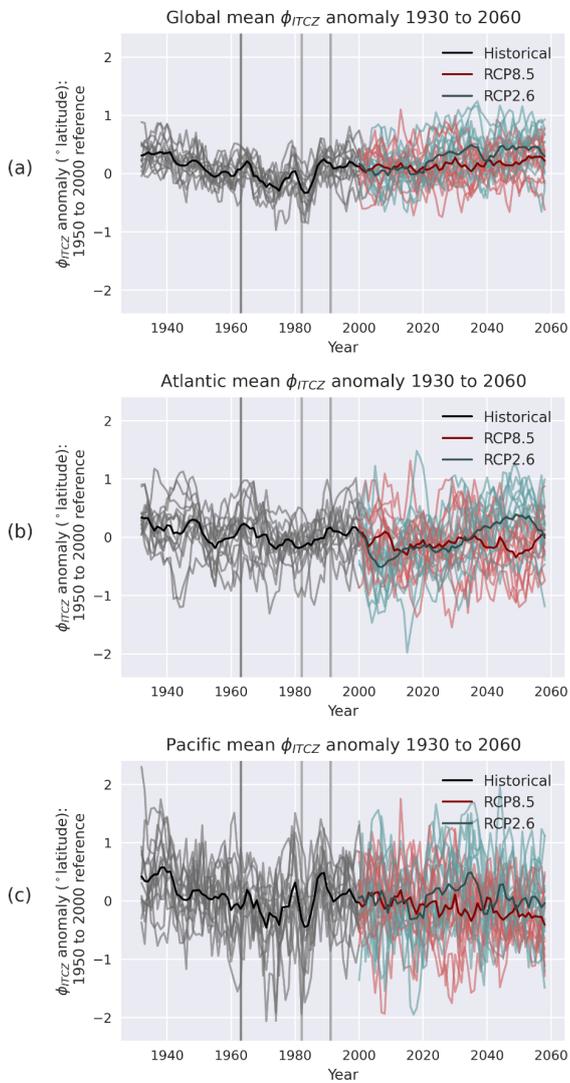
Figure 3: Time series of 5-year rolling mean Φ_{ITCZ} anomaly relative to the 1950 to 2000 reference period for (a) global, (b) Atlantic and (c) Pacific regional means. The ensemble mean time series is shown by the darker line, and the individual ensemble members in the lighter lines. Major volcanic eruptions are marked with grey vertical lines with maximum aerosol loading in the NH (El Chichón (1982, Mexico, 17.21° N) and Pinatubo (1991, Philippines, 15.08° N)) and in the SH (Mt. Agung (1963, Indonesia, 8.20° S)).
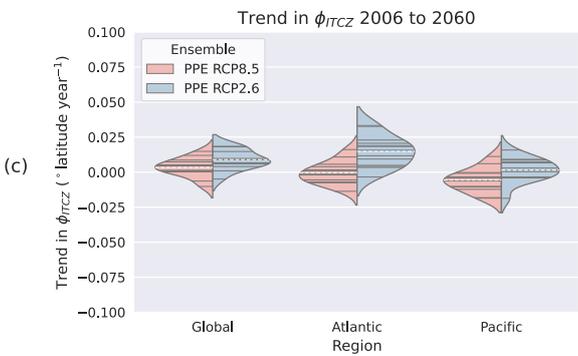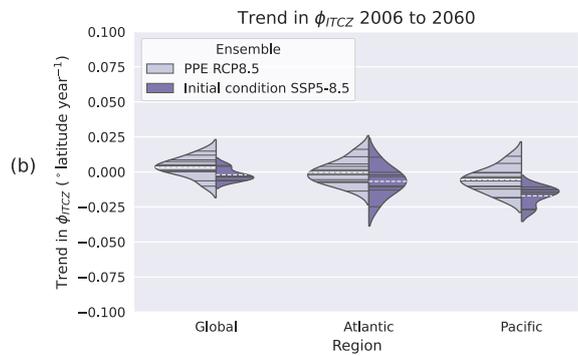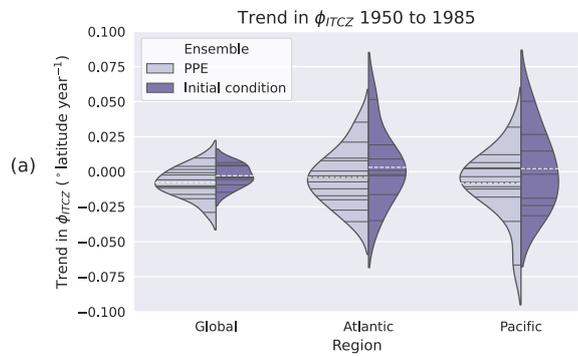
Figure 4: Trend in 5-year rolling mean Φ_{ITCZ} for (a) 1950 to 1985 and (b,c) 2006 to 2060 for global (left), Atlantic (middle) and Pacific (right) regional means. The violin plots in light purple (in b) and red (in c) are equivalent. The black lines within the violin plots show individual ensemble members (13 in the PPE, & in the initial condition ensemble) and the white dashed lines show the ensemble mean.

Figure 4(a) shows the Φ_{ITCZ} trend over 1950 to 1985 in individual ensemble members and as a density function across the PPE and initial condition ensemble. The PPE mean shows a small southward shift in the Φ_{ITCZ} throughout this time period in each region. However, across the PPE, there are both southward and northward shifts (-0.03 to 0.01 °latitude year^{-1} globally). The spread in tropical precipitation shifts over 1950 to 1985 across our single-model ensemble is comparable to that over the same period from CMIP5 (see Text S1 and Figure S4) which also displayed both south and northward shifts in tropical precipitation (Allen et al., 2015). We do not have an initial condition ensemble for each PPE member so cannot remove the effects of internal variability from each ensemble member as is common in multi-model studies. For example, in Allen et al. 2015 models that had aerosol radiative forcing experiments also had 3 to 10 ensemble members in the transient all forcing runs that were averaged to obtain the tropical precipitation shift for that model. We use the initial condition ensemble for HadGEM3-GC3.1 (a similar model version submitted to CMIP6; (Andrews et al., 2020; Murphy et al., 2018)) to estimate the spread in the Φ_{ITCZ} trend due to internal variability.

In the 1950 to 1985 global mean, the initial condition ensemble spread covers close to half (54%) of the spread in our PPE which suggests that a large fraction of our PPE spread is caused by natural variability, but there is still a considerable influence from perturbed parameters. However, regionally, the initial condition ensemble covers close to or more than the entire spread in 1950 to 1985 tropical precipitation shifts in our PPE (121% in the Atlantic, 83% in the Pacific). In previous studies, internal variability alone has been shown not to generate migrations in tropical precipitation consistent with observations over the 20th century (Chang et al., 2011; Allen et al., 2015). Whereas radiative forcing caused by anthropogenic aerosol, which predominantly cooled the Northern Hemisphere, peaking in the 1980s, has been implicated as a main driver of the migration of tropical precipitation southward up to the 1980s, followed by a northward recovery to the end of the 20th century. We note here that models incorporating both aerosol direct and indirect effects tend to better reproduce the historical changes in temperature (Booth et al., 2012; Chung and Soden, 2017) and ITCZ location (Friedman et al., 2013; Allen et al., 2015; Bonfils et al., 2020). Our single model PPE spans a range in aerosol forcing and tropical precipitation shifts comparable to multi-model studies. Therefore, we investigate the relationship between the uncertainty in the inter-hemispheric difference in aerosol forcing and tropical precipitation shifts in our PPE framework.

Figure 5 shows the relationships between Φ_{ITCZ} trend over 1950 to 1985 and the trend in inter-hemispheric (over 60 °S to 60 °N) surface air temperature (panel a), implied total radiative forcing (b) and 1860 to 1975 anthropogenic aerosol ERF (c). Figure S5 shows the corresponding plot but with inter-hemispheric variables calculated only over the ocean. A time series of inter-hemispheric temperature and AOD is shown in Figure S6 and S7. There is a strong statistical relationship (r=0.91 for global mean, r = 0.66 for regional means) between the trend in inter-hemispheric surface air temperature and the Φ_{ITCZ} trend over 1950 to 1985 (with an intercept near 0). As expected, the statistical relationship between the Φ_{ITCZ} trend and the trend in inter-hemispheric implied total forcing is also strong (r >= 0.63). An energetics framework explains how the ITCZ and corresponding latitudinal position of tropical precipitation shifts in response to changes in the inter-hemispheric distribution of energy (Kang et al., 2018b, 2008, 2009). The perturbed cross-equatorial Hadley circulation rebalances the energy asymmetry by transporting energy towards the cooler (energy deficient) hemisphere, and consequently moisture towards the warmer

555   hemisphere. As such, Figure 5(a,b) shows that ensemble members that have greater cooling in the Northern Hemisphere and a larger difference in inter-hemispheric implied total radiative forcing over 1950 to 1985 simulate stronger southward shifts in tropical precipitation. This behaviour is in line with the energetics theory of a southward migration of the ITCZ due to an energy deficient Northern hemisphere. In CMIP5, models that had a stronger inter-hemispheric aerosol radiative forcing simulated further southward shifts in tropical precipitation over 1950 to 1985, with a correlation coefficient of $r => 0.71$ across

560   13 models (Allen et al., 2015). Despite these relationships, we do not see a strong relationship between the strength of inter-hemispheric aerosol ERF estimated from the atmosphere-only runs and the degree of southward shift in tropical precipitation over 1950 to 1985 in our PPE. In the paragraphs below we evaluate several hypotheses for this weaker than expected relationship.
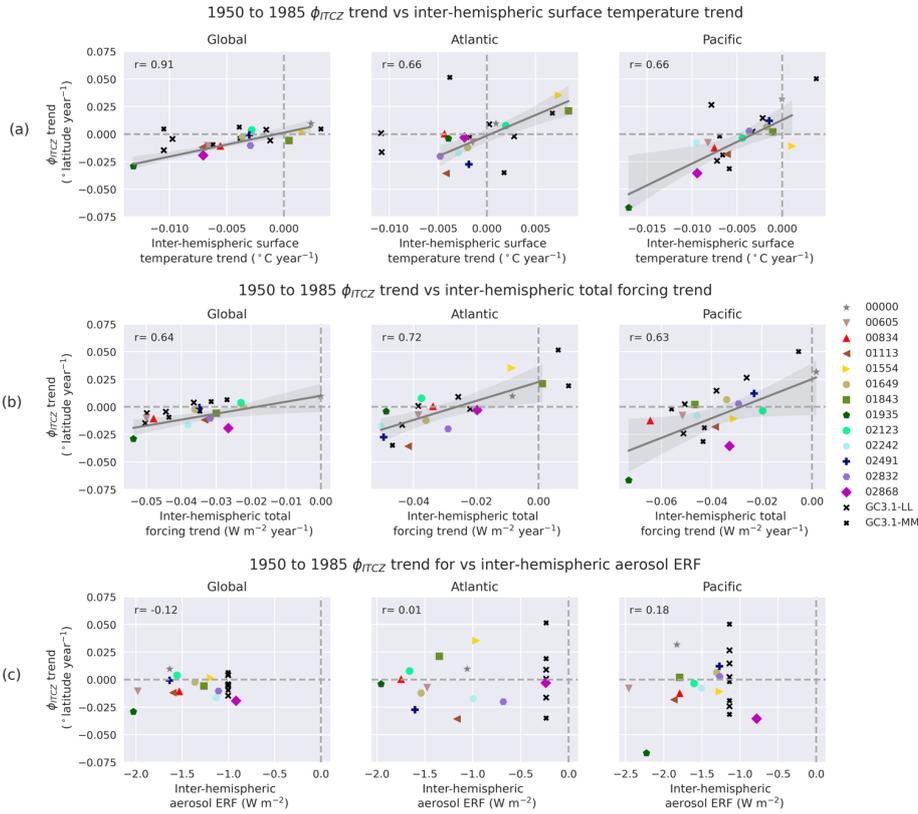
Figure 5. Scatter plot of the 1950 to 1985 trend in 5-year rolling mean Φ_{ITCZ} against the 1950 to 1985 trend in inter-hemispheric (over 60 °S to 60 °N) surface air temperature (a), implied total radiative forcing (b) and anthropogenic aerosol ERF (c) for global (left), Atlantic (middle) and Pacific (right) regional means. Anthropogenic aerosol ERF is calculated over 1860 to 1975 for the PPE, and 1850 to 2014 for the initial condition ensemble. The Spearman's rank correlation coefficient between variables is shown at top left of each plot. Trend lines are shown in plots where r > 0.5.

570
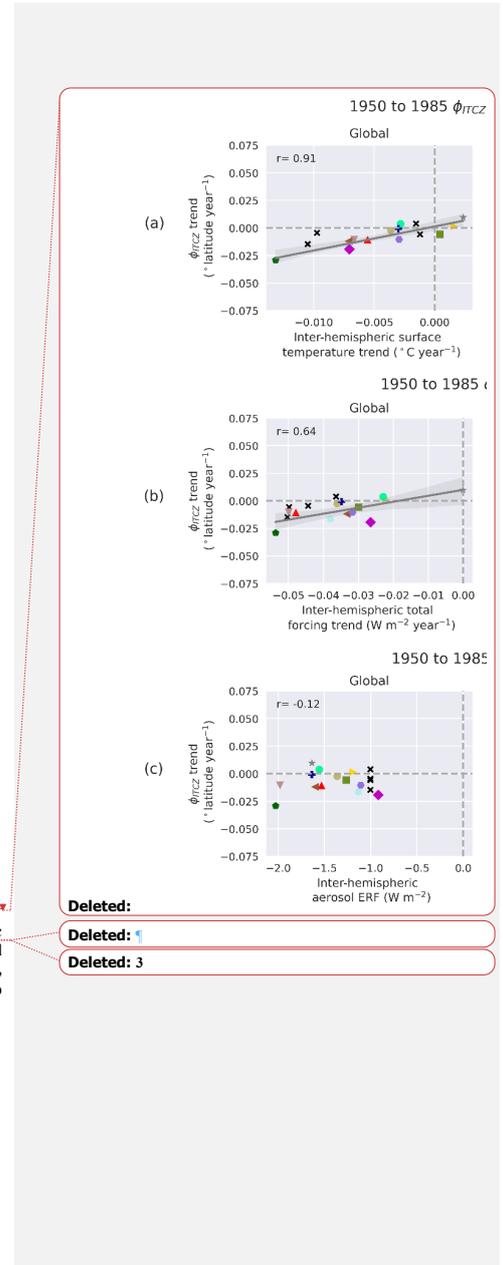
3.1.1 Potential factors obscuring a relationship between tropical precipitation shifts and anthropogenic aerosol ERF in our PPE

Figure 5(c) shows that for the initial condition ensembles of HadGEM3-GC3.1, where model realizations have the same pre-industrial to present-day aerosol forcing, a large spread in tropical precipitation shifts is possible in transient climate simulations due to internal variability. In the Atlantic region where we expect increases in aerosol emissions during 1950 to 1985 over Europe and North America to have an influence on precipitation, the spread in tropical precipitation shifts in the initial condition ensemble covers a larger range than the PPE. Hence, Figure 5(c) suggests the relationship between pre-industrial to present-day aerosol ERF and tropical precipitation shifts is obscured by internal variability in our PPE. In addition, the HadGEM3-GC3.1 initial condition ensembles cover nearly all (88% in the global mean) of the spread in the trend in the inter-hemispheric difference in temperature our PPE, which may be the reason why there is also only a weak relationship between the trend in the inter-hemispheric difference in temperature during the 20th century and 1860 to 1975 anthropogenic aerosol ERF (Figure S8). If we had an initial condition ensemble for each PPE member or a larger sample size, the expected relationships may have emerged more strongly. The effect of internal variability is therefore likely one of the main reasons why there is not a relationship between inter-hemispheric aerosol forcing and tropical precipitation shifts over the 20th century in our ensemble.

The strength of relationships between the Φ_{ITCZ} trend and inter-hemispheric variables are also sensitive to the time period chosen, as shown in Table 1. The 1950 to 1985 time period which has the strongest relationship between tropical precipitation shifts and both inter-hemispheric temperature and implied total forcing trends encapsulates two major volcanic eruptions. There is a weaker correlation in the longer time series or the time series excluding El Chichón. These results may indicate that volcanic rather than anthropogenic aerosol changes drive much of the coherent changes in inter-hemispheric temperature trends, implied total forcing trend, and tropical precipitation shifts during 1950 to 1985. However, the lack of a strong relationship between tropical precipitation shifts and historical anthropogenic aerosol ERF is unlikely to be related to the choice of analysis period as there is little evidence of stronger correlations with anthropogenic aerosol ERF estimates on other 20th century timescales.

The anthropogenic aerosol ERF is quantified as the radiative change between two periods (1860 to 1975) using atmosphere-only simulations with SSTs and other climate forcers prescribed for 2005 to 2009. As such, the anthropogenic aerosol ERF might not be representative of the aerosol-driven climate response in transient climate simulations due to the differences in time period, mediation of aerosol radiative effects by the coupling of ocean processes and evolution of other climate forcers, and/or internal variability (Voigt et al., 2017). Firstly, to investigate further we examined the relationship between Φ_{ITCZ} trend and time evolving variables related to aerosol radiative effects, as shown in Table 2. Over 1950 to 1985, there is no clear relationship between the trend in Φ_{ITCZ} and the trend in the inter-hemispheric difference of either outgoing shortwave radiation at TOA (Figure S7) or total AOD (Figure S10). There is some suggestion of a relationship between tropical precipitation shifts and the trend in the inter-hemispheric difference of both shortwave non-cloud radiative effect (Figure S11) and dust AOD (Figure S10), although these variables can also be affected by internal variability. These results with the time-evolving

variables do not clarify how representative pre-industrial to 1975 aerosol ERF is of transient aerosol radiative effects in the coupled simulations. Secondly, studies have shown that the slow precipitation response to aerosol forcing is a more effective driver of ITCZ shifts than the fast precipitation response (Voigt et al., 2017; Zhang et al., 2021). By definition aerosol ERF does not quantity the climate response to aerosol-mediated surface temperature changes, and hence alongside the time-evolving variables related to aerosol radiative effects, may not be a useful proxy for aerosol-driven slow precipitation changes (which occur through surface temperature change). However, such a line of thinking does not explain the difference between our results and those from a multi-model ensemble (Allen et al. 2015).

Time period	Correlation with the trend in inter-hemispheric surface air temperature (°C year^{-1})	Correlation with the trend in inter-hemispheric implied total forcing (W m^{-2} year^{-1})	Correlation with inter-hemispheric 1860 to 1975 anthropogenic aerosol ERF (W m^{-2})
1950 to 1985 (shown)	r= 0.91	r= 0.64	r= -0.12
1950 to 1980	r= 0.56	r= 0.65	r= -0.04
1940 to 1985	r= 0.29	r= 0.48	r= -0.12
1940 to 1980	r= -0.01	r= 0.57	r= -0.07
1940 to 1975	r= 0.19	r= 0.77	r= -0.30

Table 1: Table of Spearman's rank correlation coefficients for the trend in global mean 5-year rolling mean Φ_{ITCZ} and global inter-hemispheric (60 °S to 60 °N) variables shown in Figure 5 with values for alternate time periods.

Variable	Correlation with Φ_{ITCZ} trend (° latitude year^{-1})
Trend in inter-hemispheric total AOD (year^{-1})	r= -0.23
Trend in inter-hemispheric dust AOD (year^{-1})	r= -0.54
Trend in inter-hemispheric shortwave non-cloud radiative effect (W m^{-2} year^{-1})	r= 0.54
Trend in inter-hemispheric shortwave cloud radiative effect (W m^{-2} year^{-1})	r= -0.34
Trend in inter-hemispheric top of atmosphere outgoing shortwave flux (W m^{-2} year^{-1})	r=-0.34

Table 2: Table of Spearman's rank correlation coefficients for the 1950 to 1985 trend in global mean 5-year rolling mean Φ_{ITCZ} and additional global inter-hemispheric (60 °S to 60 °N) variables.

Our 13 PPE members include the combined effects of perturbations to 8 parameters in the aerosol model, alongside many parameters in the physical atmosphere model. So in our PPE, any relationship between anthropogenic aerosol radiative forcing and tropical precipitation might be masked by the effect of perturbations to physical atmosphere parameters. The strongest correlations between the Φ_{ITCZ} trend over 1950 to 1985 and individual perturbed parameters in our PPE are shown in Figure S12. Some of these relationships may be indicative of important atmospheric parameter effects on tropical precipitation shifts. For example, (Kang et al., 2008, 2009) showed how tuning a convective parameter related to entrainment can alter cloud radiative properties and cause a range in magnitude of ITCZ shifts for a given inter-hemispheric thermal forcing. In our PPE, the parameter that controls shallow convective core radiative effects (cca_sh_knob) and the parameter that controls the sensitivity of mid-level convection to relative humidity and entrainment (ent_fac_md) have a relationship with the Φ_{ITCZ} trend over some regions. Hence, both these parameters could modulate the sensitivity of ITCZ shifts through altering cloud radiative feedbacks. In the global and Atlantic means, the scaling of natural dimethyl sulphide emissions flux (ps_natl_dms_emiss), which could alter the hemispheric contrast of aerosol forcing, has a relationship with the Φ_{ITCZ} trend. Parameters from the land surface (related to soil moisture thresholds; psm, and altering the temperature dependence of photosynthesis; tupp_io) and the cloud microphysics (aspect ratio of ice particles; ar) scheme also have a relationship with Φ_{ITCZ} trend over some regions. These results are at best indications of possible parameter effects. Our correlations are calculated using only 13 ensemble members that conflate the uncertainty in 47 model parameters. So, further simulations would be needed to clarify parametric effects on tropical precipitation shifts. In addition, in the Atlantic and Pacific regions the uncertainty in tropical precipitation shifts due to internal variability may be larger than parametric model uncertainty, so to more robustly quantify the effects of parameters we would need initial condition ensembles for each parameter combinations of the 47 uncertain model parameters.

Overall, our analysis of 20th century latitudinal shifts in tropical precipitation shows that any relationship between these shifts and the hemispheric contrast in 1860 to 1975 anthropogenic aerosol ERF is difficult to detect when accounting for the effect of parametric model uncertainty and internal variability. The latitudinal shift of tropical precipitation over 1950 to 1985 is, however, associated with the trend in inter-hemispheric surface temperature and implied total radiative forcing. It is also clear that major volcanic eruptions in the 20th century induced relatively short-lived shifts in tropical precipitation and contribute to a time-period dependence of the strength of these relationships.

3.2 Tropical Precipitation Shifts Up To Mid-21st Century

Here, we examine the relationship between the Φ_{ITCZ} trend and our inter-hemispheric variables over 2006 to 2060 under emission scenarios RCP8.5 and RCP2.6. The reductions in anthropogenic aerosol emissions and consequential warming of the northern hemisphere in the 21st century have been projected to cause a northward shift in the position of ITCZ and tropical precipitation (Hwang et al., 2013; Allen, 2015). Although the warming caused by increasing CO_2 emissions is more homogeneous, it can also lead to a migration in the position of the ITCZ and tropical precipitation. For example, climate responses to GHG-induced warming such as ice-albedo feedbacks, the land-dominated Northern Hemisphere warming, cloud

710 and ocean heat content changes may lead to a northward shift in the ITCZ, whereas responses such as AMOC weakening and enhanced longwave cooling may lead to a southward shift (McFarlane and Frierson, 2017). These drivers of tropical precipitation shifts in the 21st century will also act on different timescales. Results from multi-model studies have mixed conclusions on how zonal mean tropical precipitation will migrate in the future.

Figure 3 shows the 5-year rolling mean evolution of Φ_{ITCZ} up to 2060 across our PPE. For scenario RCP8.5, the ensemble
715 mean Φ_{ITCZ} remains steady globally and in the Atlantic up to mid-21st century, with a slight southward migration in the Pacific. For RCP2.6, there is a northward migration of Φ_{ITCZ} up to mid-century globally and in the Atlantic, followed by a southward migration from 2050 to 2060. Yet in the Pacific, the northward migration ends in around 2035 and is followed by a strong, but brief southward migration. The Φ_{ITCZ} exhibits greater variability in scenario RCP2.6, which is most pronounced in the Pacific.

Figure 4(b.c) shows the Φ_{ITCZ} trend over 2006 to 2060 across individual members in our PPE and as a density function. Figure
720 4(b) also shows an estimate of the impact of internal variability (superimposed on a forced signal) over the same period using the initial condition ensemble of HadGEM3-GC3.1 under emission scenario SSP5-8.5. The total radiative forcing levels at 2100 are designed to be the same in RCP8.5 and SSP5-8.5 but there are differences in the emissions scenarios of individual forcing agents (Gidden et al., 2019), which could affect the evolution of tropical precipitation shifts. Under RCP8.5, the PPE mean shows only a small change in Φ_{ITCZ}, with both north and southward migrations in Φ_{ITCZ} across the ensemble. Hence, we
725 find no robust evidence of a tropical precipitation shifts under RCP8.5 by mid-21st century, which is in agreement with the conclusions based on end-of-century ITCZ shifts in (Byrne et al., 2018b). The spread in Φ_{ITCZ} trend due to internal variability under SSP5-8.5 in the initial condition ensemble is smaller than under RCP8.5 in our PPE globally and in the Pacific, but comparable in the Atlantic region. Figure 4(c) contrasts the Φ_{ITCZ} trend over 2006 to 2060 between RCP8.5 and RCP2.6 scenarios. By mid-century, tropical precipitation shifts further northward in RCP2.6, compared to RCP8.5. This northward
730 migration in tropical precipitation for RCP2.6 is in line with Allen (2015), prior to the then southward shift between mid and end of the 21st century. The largest difference in tropical precipitation shift between emission scenarios is in the Atlantic, which may be related to scenario dependence of AMOC strength. The AMOC is projected to weaken under warming (Schleussner et al., 2014; Collins et al., 2019) and as AMOC weakening is likely to reduce a northward ITCZ shift (McFarlane and Frierson, 2017), the effect would be more dominant in RCP8.5 than RCP2.6 due to the greater warming from increasing GHG emissions
735 combined with warming from anthropogenic aerosol emission reductions. In addition, the strength of the AMOC over the 20th century has been linked to the strength of aerosol forcing and thus aerosol forcing may also affect future projections (Menary et al., 2020; Hassan et al., 2021). Hence, the further northward migration of tropical precipitation up to 2060 in RCP2.6 in our ensemble is likely due to a combination of greater anthropogenic aerosol emission reductions in RCP2.6 compared to RCP8.5, and a greater dominance of processes in RCP8.5 that pull tropical precipitation southwards. For example, the slight southward
740 migration of Φ_{ITCZ} in the Pacific could be due to weakening of the Walker circulation causing, in the eastern tropical Pacific Ocean, a regional southward shift of the ITCZ (Mamalakis et al., 2021). We note here that in both emission scenarios, the spread in Φ_{ITCZ} trend across the near-term future ensembles is smaller than over the historical period, due to the trend being

calculated over a longer time period. A shorter future time period induces a larger spread in the Φ_{ITCZ} trend across the PPE (Figure S13), which is comparable the spread in the historical period.

Figure 6 shows the relationship between our inter-hemispheric variables and the Φ_{ITCZ} trend over 2006 to 2060 in RCP2.6 and RCP8.5. Figure S14 shows a corresponding figure with inter-hemispheric variables calculated only over the ocean. The top panel of Figure 6 shows that there is a relationship between the Φ_{ITCZ} trend and the trend in inter-hemispheric surface temperature in each of the RCP ensembles (consistent to what we find for the historical period). For each of the RCP scenario ensembles the relationship between the global Φ_{ITCZ} trend and the trend in inter-hemispheric surface temperature is stronger than we found in the longer historical trends (Table 1), but weaker than those beginning in 1950 which were most affected by volcanic eruptions (Figure 5). Contrary to the historical period, we identify a relationship between the Φ_{ITCZ} trend over 2006 to 2060 and inter-hemispheric 1860 to 2005 aerosol ERF in the Pacific under RCP8.5 (r=-0.69). Emission reductions in Asia will dominate future global reductions in anthropogenic aerosol emissions (Lund et al., 2019), and align with our results that there is a strong relationship between the magnitude of inter-hemispheric aerosol ERF and tropical precipitation shifts, particularly in the Pacific region. However, the lower latitude of emission reductions over Asia, in comparison to Europe or North America, may affect the sensitivity of the ITCZ shift. There is no relationship in the Atlantic, and consequently the global mean response (r= -0.47) is weaker than the Pacific. Figure S8 shows there is also a suggestion of a relationship between the inter-hemispheric temperature trend and 1860 to 2005 aerosol ERF in the Pacific, which is slightly stronger over the ocean (not shown). These results show that in our PPE, ensemble members that have a stronger difference in inter-hemispheric aerosol ERF over the industrial period, and more warming in the Northern hemisphere in the near-term future under scenario RCP8.5, simulate further northward migrations in tropical precipitation, particularly in the Pacific region. It is surprising, however, that there is no clear relationship between the Φ_{ITCZ} trend and inter-hemispheric aerosol ERF in RCP2.6, where we expected faster aerosol emission reductions to yield a clearer tropical precipitation response. Possible causes of a stronger relationship between tropical precipitation shifts and aerosol radiative forcing under RCP8.5 could be due to feedbacks between warming and aerosol radiative forcing. For example, aerosol residence times and associated net radiative effects may increase in a warmer climate (Bellouin et al., 2011; Takemura, 2020) which may amplify the effect of anthropogenic aerosol forcing on ITCZ position in RCP8.5 compared to RCP2.6.

Our analysis of 21st century tropical precipitation shifts suggests that the uncertainty in the inter-hemispheric difference in aerosol ERF contributes to the spread of projected tropical precipitation shifts across our ensemble in the near-term future under RCP8.5. This is especially the case in the Pacific regional mean, as near-term future aerosol reduction will be driven by reductions from Asia. Our analysis of the historical period showed that the position of tropical precipitation can be strongly modulated by major volcanic eruptions that lead to inter-hemispheric differences in temperature. Hence, any predictive skill for future shifts in tropical precipitation will also be limited by the effect of any future major volcanic eruptions that induce differences in hemispheric energy balance.

Figure 6: Scatter plot of trend in 5-year rolling mean Φ_{ITCZ} in 2006 to 2060 against the trend in inter-hemispheric (60 °S-60 °N) surface air temperature (a), and 1860 to 2005 anthropogenic aerosol ERF (b, c) for global (left), Atlantic (middle) and Pacific regional means (right). The Spearman's rank correlation coefficient is shown at top left of each plot. Trends lines are shown when r > 0.5.

805

4. Conclusion

The inter-hemispheric nature of anthropogenic aerosol radiative forcing associated with evolving anthropogenic aerosol emissions has been linked to driving tropical precipitation shifts during the latter half of the 20th century and over the 21st century (Allen, 2015; Allen et al., 2015; Hwang et al., 2013; Chang et al., 2011; Rotstayn et al., 2015; Chemke and Dagan, 2018). In the CMIP5 multi-model ensemble there is a strong correlation between the strength of pre-industrial to present-day inter-hemispheric aerosol forcing and the latitudinal shift in tropical precipitation over 1950 to 1985 (Allen et al., 2015). We have used a perturbed parameter ensemble of the HadGEM3-GC3.05 climate model that spans a range of aerosol forcing comparable to current generation climate models to further investigate the relationship between anthropogenic aerosol forcing and tropical precipitation shifts.

In the 20th century as anthropogenic aerosol emissions increased, our PPE mean shows a long-term southward migration in the latitudinal position of tropical precipitation globally and in the Atlantic and Pacific up to around 1985 (e.g. 0.01 °latitude year^{-1} globally over 1940 to 1985). Over the 20th century there are also brief shifts in tropical precipitation in response to major volcanic eruptions. Of the time periods we analysed, the 1950 to 1985 time period which encapsulates two major volcanic eruptions, had the strongest relationship between tropical precipitation shifts and the hemispheric contrast in temperature and implied total radiative forcing over the same period (i.e. ensemble members with more cooling in the Northern Hemisphere simulated a further southward shift of the ITCZ). Both the long-term trends and the rapid response to volcanic eruptions are in-line with the theoretical energetic framework and modelling studies that have shown the zonal mean position of the ITCZ and corresponding tropical precipitation migrates in response to an anomalous inter-hemispheric energy balance (Kang et al., 2018b).

Despite a contemporaneous relationship between tropical precipitation shifts and the trend in the inter-hemispheric difference in temperature and implied total forcing, we find no statistically significant relationship between the strength of inter-hemispheric 1860 to 1975 anthropogenic aerosol ERF and the magnitude of tropical precipitation shifts in the PPE over the 20th century, which contradicts results from CMIP5 (Allen et al., 2015). We propose multiple hypotheses for this different result. Overall, our results suggest that being unable to isolate forced changes from those due to internal variability (due to an absence of initial condition ensembles of our PPE members) and accounting for single-model uncertainty obscure the role of anthropogenic aerosol forced responses in our ensemble over the 20th century.

Drivers of future tropical precipitation shifts are harder to disentangle, as both forced responses and climate feedbacks due to warming will have a bearing on the direction and magnitude of ITCZ shifts over the 21st century (McFarlane and Frierson, 2017). In the near-term future (up to 2060) globally our ensemble mean shows a negligible migration in tropical precipitation in RCP8.5, and a further northward migration in tropical precipitation in RCP2.6. The further northward migration in RCP2.6 compared to RCP8.5 is likely due to a combination of a faster reduction of anthropogenic aerosol emissions, in combination with warming-induced feedbacks (such as AMOC weakening) having a greater modulation of the regional ITCZ position in

RCP8.5. We do find ensemble members that have a stronger positive trend in inter-hemispheric temperature and forcing (i.e. due to more warming in the Northern Hemisphere) simulate further northward migrations in tropical precipitation.

850 In contrast to the historical time period, we find a relationship between the strength of inter-hemispheric 1860 to 2005 anthropogenic aerosol ERF (which we use as a proxy of present-day aerosol influence) and future tropical precipitation shifts under RCP8.5. This relationship is strongest in the Pacific where Asian anthropogenic aerosols have a strong historical and future influence. On the premise that present day anthropogenic aerosol influence is informative about future anthropogenic aerosol influence, this indicates ensemble members with a large hemispheric difference in historical aerosol radiative forcing,

855 will have a further northward tropical precipitation shift in response to future aerosol reductions. Faster anthropogenic aerosol emission reductions is likely one of the factors why RCP2.6 has a further northward shift in tropical precipitation by mid-21st century than RCP8.5. Yet, it is surprising that this logic does not follow through to there being a stronger relationship between tropical precipitation shifts and aerosol forcing in RCP2.6, suggesting climate feedbacks due to warming can influence the sensitivity of the climate response to aerosol forcing (Takemura, 2020; Nazarenko et al., 2017).

860 Overall, our study suggests the persistent uncertainty in aerosol ERF plays a role in how accurately we can project zonal mean tropical precipitation shifts in the near-term future under RCP8.5. However, any predictive skill for future tropical precipitation shifts will also be limited by the effect of future major volcanic eruptions that can temporarily shift tropical precipitation. Our study presents open questions on the role of anthropogenic aerosol radiative forcing in modulating tropical precipitation shifts over the historical and future periods in climate models, which we cannot definitively answer here because our experiment is

865 designed to sample single-model uncertainty and thus has a relatively small sample size and neglects the effects of internal variability. Additional experiments that clarify the role of aerosols on near-term future tropical precipitation shifts are also needed. In a broader analysis involving multi-model and other single-model ensembles we could further develop our understanding of the relationship between feedbacks due to warming, future aerosol forcing and tropical precipitation shifts up to mid-21st century across multiple emission scenarios. Hence, we suggest future work investigating the role between

870 aerosol forcing and tropical precipitation shifts in the CMIP6 multi-model ensemble and other single-model ensembles that span a range of aerosol radiative forcing values.

875

Data and code availability

880 The gridded global precipitation and temperature data for the historical and RCP8.5 HadGEM3-GC3.05 PPE simulations used in this study is available in the CEDA Archive (https://catalogue.ceda.ac.uk/uuid/97bc0c622a24489aa105f5b8a8efa3f0). Gridded global data for HadGEM3GC3.1 that was submitted to CMIP6 is available to download (https://esgf-index1.ceda.ac.uk/). The historical simulations are available under CMIP DECK and future SSP5-8.5 under ScenarioMIP. The model Source ID is HadGEM3-GC31-LL (Ridley et al., 2019a). The four members of each historical ensemble are identified

885 by the following Variant Labels: r1i1p1f3 to r4i1p1f3. Simplified data and code required to reproduce the main figures in this article will be provided on Zonodo (link placeholder). All other underlying datasets generated during and/or analysed during the current study are available from the Met Office Hadley Centre on reasonable request.

Author contribution

AP, BB, LR, KC designed the idea for this study. The analysis of data and figure preparation were completed by the AP. BB,
890 DS and JR extracted data and performed additional aerosol forcing simulations for the HadGEM3-GC3.05 PPE. All co-authors provided discussion on the interpretation of results. AP wrote the manuscript with advice from all co-authors.

Competing interests

The authors declare that they have no conflict of interest.

Acknowledgments

895 AP was funded by a doctoral training grant from the Natural Environment Research Council (NERC) with a CASE studentship with the Met Office Hadley Centre under grant no. NE/P010547/1. LR and KC receiving funding from NERC under grant nos. NE/J024252/1 (GASSP) and NE/P013406/1 (A-CURE). LR and KC received funding from the European Union's Horizon 2020 research and innovation programme under grant agreement no. 821205 (the FORCeS project). BB, DS were supported by the Met Office Hadley Centre Climate Programme funded by BEIS. JR was supported by the UK-China Research &
900 Innovation Partnership Fund through the Met Office Climate Science for Service Partnership (CSSP) China as part of the Newton Fund. The work contribution of CB was performed under the auspices of the US Department of Energy (DOE) by Lawrence Livermore National Laboratory under contract no. DE-AC52–07NA27344. CB was also supported by the DOE Regional and Global Model Analysis Program under the PCMDI SFA. The JASMIN facility (www.jasmin.ac.uk/) via the Centre for Environmental Data Analysis was used for data processing, which is funded by NERC and the UK Space Agency
905 and delivered by the Science and Technology Facilities Council.

References

Ackerley, D., Booth, B. B. B., Knight, S. H. E., Highwood, E. J., Frame, D. J., Allen, M. R., and Rowell, D. P.: Sensitivity of Twentieth-Century Sahel Rainfall to Sulfate Aerosol and CO2 Forcing, Journal of Climate, 24, 4999–5014, https://doi.org/10.1175/JCLI-D-11-00019.1, 2011.

Allen, R. J.: A 21st century northward tropical precipitation shift caused by future anthropogenic aerosol reductions, Journal of Geophysical Research, 120, 9087–9102, https://doi.org/10.1002/2015JD023623, 2015.

Allen, R. J., Evan, A. T., and Booth, B. B. B.: Interhemispheric aerosol radiative forcing and tropical precipitation shifts during the late Twentieth Century, Journal of Climate, 28, 8219–8246, https://doi.org/10.1175/JCLI-D-15-0148.1, 2015.

Andrews, M. B., Ridley, J. K., Wood, R. A., Andrews, T., Blockley, E. W., Booth, B., Burke, E., Dittus, A. J., Florek, P., Gray, L. J., Haddad, S., Hardiman, S. C., Hermanson, L., Hodson, D., Hogan, E., Jones, G. S., Knight, J. R., Kuhlbrodt, T., Misios, S., Mizielinski, M. S., Ringer, M. A., Robson, J., and Sutton, R. T.: Historical Simulations With HadGEM3-GC3.1 for CMIP6, Journal of Advances in Modeling Earth Systems, 12, e2019MS001995, https://doi.org/10.1029/2019MS001995, 2020.

Andrews, T., Andrews, M. B., Bodas-Salcedo, A., Jones, G. S., Kuhlbrodt, T., Manners, J., Menary, M. B., Ridley, J., Ringer, M. A., Sellar, A. A., Senior, C. A., and Tang, Y.: Forcings, Feedbacks, and Climate Sensitivity in HadGEM3-GC3.1 and UKESM1, Journal of Advances in Modeling Earth Systems, 11, 4377–4394, https://doi.org/10.1029/2019MS001866, 2019.

Atwood, A. R., Donohoe, A., Battisti, D. S., Liu, X., and Pausata, F. S. R.: Robust Longitudinally Variable Responses of the ITCZ to a Myriad of Climate Forcings, Geophysical Research Letters, 47, e2020GL088833, https://doi.org/https://doi.org/10.1029/2020GL088833, 2020.

Bellouin, N., Rae, J., Jones, A., Johnson, C., Haywood, J., and Boucher, O.: Aerosol forcing in the Climate Model Intercomparison Project (CMIP5) simulations by HadGEM2-ES and the role of ammonium nitrate, Journal of Geophysical Research, 116, D20206, https://doi.org/10.1029/2011JD016074, 2011.

Bellouin, N., Quaas, J., Gryspeerdt, E., Kinne, S., Stier, P., Watson-Parris, D., Boucher, O., Carslaw, K. S., Christensen, M., Daniau, A. L., Dufresne, J. L., Feingold, G., Fiedler, S., Forster, P., Gettelman, A., Haywood, J. M., Lohmann, U., Malavelle, F., Mauritsen, T., McCoy, D. T., Myhre, G., Mülmenstädt, J., Neubauer, D., Possner, A., Rugenstein, M., Sato, Y., Schulz, M., Schwartz, S. E., Sourdeval, O., Storelvmo, T., Toll, V., Winker, D., and Stevens, B.: Bounding Global Aerosol Radiative Forcing of Climate Change, https://doi.org/10.1029/2019RG000660, 1 March 2020.

Biasutti, M. and Giannini, A.: Robust Sahel drying in response to late 20th century forcings, Geophysical Research Letters, 33, https://doi.org/https://doi.org/10.1029/2006GL026067, 2006.

Bonfils, C. J. W., Santer, B. D., Fyfe, J. C., Marvel, K., Phillips, T. J., and Zimmerman, S. R. H.: Human influence on joint changes in temperature, rainfall and continental aridity, Nature Climate Change, 1–6, https://doi.org/10.1038/s41558-020-0821-1, 2020.

Booth, B. B. B., Dunstone, N. J., Halloran, P. R., Andrews, T., and Bellouin, N.: Aerosols implicated as a prime driver of twentieth-century North Atlantic climate variability, Nature, 484, 228–232, https://doi.org/10.1038/nature10946, 2012.

Broccoli, A. J., Dahl, K. A., and Stouffer, R. J.: Response of the ITCZ to Northern Hemisphere cooling, Geophysical Research Letters, 33, https://doi.org/10.1029/2005GL024546, 2006.

Byrne, M. P., Pendergrass, A. G., Rapp, A. D., and Wodzicki, K. R.: Response of the Intertropical Convergence Zone to Climate Change: Location, Width, and Strength, Current Climate Change Reports, 4, 355–370, https://doi.org/10.1007/s40641-018-0110-5, 2018a.

Byrne, M. P., Pendergrass, A. G., Rapp, A. D., and Wodzicki, K. R.: Response of the Intertropical Convergence Zone to Climate Change: Location, Width, and Strength, https://doi.org/10.1007/s40641-018-0110-5, 9 December 2018b.

Chang, C. Y., Chiang, J. C. H., Wehner, M. F., Friedman, A. R., and Ruedy, R.: Sulfate aerosol control of tropical atlantic climate over the twentieth century, Journal of Climate, 24, 2540–2555, https://doi.org/10.1175/2010JCLI4065.1, 2011.

Chemke, R. and Dagan, G.: The effects of the spatial distribution of direct anthropogenic aerosols radiative forcing on atmospheric circulation, Journal of Climate, 31, 7129–7145, https://doi.org/10.1175/JCLI-D-17-0694.1, 2018.

Chiang, J. C. H. and Bitz, C. M.: Influence of high latitude ice cover on the marine Intertropical Convergence Zone, Climate Dynamics, 25, 477–496, https://doi.org/10.1007/s00382-005-0040-5, 2005.

Chiang, J. C. H. and Friedman, A. R.: Extratropical cooling, interhemispheric thermal gradients, and tropical climate change, Annual Review of Earth and Planetary Sciences, 40, 383–412, https://doi.org/10.1146/annurev-earth-042711-105545, 2012.

Choudhury, B. A., Rajesh, P. V., Zahan, Y., and Goswami, B. N.: Evolution of the Indian summer monsoon rainfall simulations from CMIP3 to CMIP6 models, Climate Dynamics, 1–26, https://doi.org/10.1007/s00382-021-06023-0, 2021.

Chung, E. S. and Soden, B. J.: Hemispheric climate shifts driven by anthropogenic aerosol-cloud interactions, Nature Geoscience, https://doi.org/10.1038/NGEO2988, 2017.

Collins, M., Sutherland, M., Bouwer, L., Cheong, S.-M., Frölicher, T., Combes, H. J. Des, Roxy, M. K., Losada, I., McInnes, K., Ratter, B., Rivera-Arriaga, E., Susanto, R. D., Swingedouw, D., and Tibig, L.: Extremes, Abrupt Changes and Managing Risk. In: IPCC Special Report on the Ocean and Cryosphere in a Changing Climate, 2019.

Colose, C. M., LeGrande, A. N., and Vuille, M.: The influence of volcanic eruptions on the climate of tropical South America during the last millennium in an isotope-enabled general circulation model, Climate of the Past, 12, 961–979, https://doi.org/10.5194/cp-12-961-2016, 2016.

Diao, C., Xu, Y., and Xie, S.-P.: Anthropogenic aerosol effects on tropospheric circulation and sea surface temperature (1980–2020): separating the role of zonally asymmetric forcings, Atmospheric Chemistry and Physics, 21, 18499–18518, https://doi.org/10.5194/acp-21-18499-2021, 2021.

Dong, B., Sutton, R. T., Highwood, E., and Wilcox, L.: The impacts of European and Asian anthropogenic sulfur dioxide emissions on Sahel rainfall, Journal of Climate, 27, 7000–7017, https://doi.org/10.1175/JCLI-D-13-00769.1, 2014.

Donohoe, A., Marshall, J., Ferreira, D., and Mcgee, D.: The relationship between ITCZ location and cross-equatorial atmospheric heat transport: From the seasonal cycle to the last glacial maximum, Journal of Climate, 26, 3597–3618, https://doi.org/10.1175/JCLI-D-12-00467.1, 2013.

Evans, S., Dawson, E., and Ginoux, P.: Linear Relation Between Shifting ITCZ and Dust Hemispheric Asymmetry, Geophysical Research Letters, 47, e2020GL090499, https://doi.org/https://doi.org/10.1029/2020GL090499, 2020.

Forster, P., Storelvmo, T., Armour, K., Collins, W., Dufresne, J.-L., Frame, D., Lunt, D. J., Mauritsen, T., Palmer, M. D., Watanabe, M., Wild, M., and Zhang, H.: The Earth's Energy Budget, Climate Feedbacks, and Climate Sensitivity. In Climate Change 2021: The Physical Science Basis. Contribution of Working Group I to the Sixth Assessment Report of the Intergovernmental Panel on Climate Change, 2021.

Friedman, A. R., Hwang, Y.-T., Chiang, J. C. H., and Frierson, D. M. W.: Interhemispheric Temperature Asymmetry over the Twentieth Century and in Future Projections, Journal of Climate, 26, 5419–5433, https://doi.org/10.1175/JCLI-D-12-00525.1, 2013.

Frierson, D. M. W. and Hwang, Y. T.: Extratropical influence on ITCZ shifts in slab ocean simulations of global warming, Journal of Climate, 25, 720–733, https://doi.org/10.1175/JCLI-D-11-00116.1, 2012.

Giannini, A. and Kaplan, A.: The role of aerosols and greenhouse gases in Sahel drought and recovery, Climatic Change, 152, 449–466, https://doi.org/10.1007/s10584-018-2341-9, 2019.

Gidden, M. J., Riahi, K., Smith, S. J., Fujimori, S., Luderer, G., Kriegler, E., Van Vuuren, D. P., Van Den Berg, M., Feng, L., Klein, D., Calvin, K., Doelman, J. C., Frank, S., Fricko, O., Harmsen, M., Hasegawa, T., Havlik, P., Hilaire, J., Hoesly, R., Horing, J., Popp, A., Stehfest, E., and Takahashi, K.: Global emissions pathways under different socioeconomic scenarios for use in CMIP6: A dataset of harmonized emissions trajectories through the end of the century, Geoscientific Model Development, 12, 1443–1475, https://doi.org/10.5194/gmd-12-1443-2019, 2019.

Green, B. and Marshall, J.: Coupling of Trade Winds with Ocean Circulation Damps ITCZ Shifts, Journal of Climate, 30, 4395–4411, https://doi.org/10.1175/JCLI-D-16-0818.1, 2017.

Green, B., Marshall, J., and Donohoe, A.: Twentieth century correlations between extratropical SST variability and ITCZ shifts, Geophysical Research Letters, 44, 9039–9047, https://doi.org/https://doi.org/10.1002/2017GL075044, 2017.

Gregory, J. M. and Forster, P. M.: Transient climate response estimated from radiative forcing and observed temperature change, Journal of Geophysical Research Atmospheres, 113, D23105, https://doi.org/10.1029/2008JD010405, 2008.

Hassan, T., Allen, R. J., Liu, W., and Randles, C. A.: Anthropogenic aerosol forcing of the Atlantic meridional overturning circulation and the associated mechanisms in CMIP6 models, Atmospheric Chemistry and Physics, 21, 5821–5846, https://doi.org/10.5194/acp-21-5821-2021, 2021.

Haywood, J. M., Jones, A., Bellouin, N., and Stephenson, D.: Asymmetric forcing from stratospheric aerosols impacts Sahelian rainfall, Nature Climate Change, 3, 660–665, https://doi.org/10.1038/nclimate1857, 2013.

Herman, R. J., Giannini, A., Biasutti, M., and Kushnir, Y.: The effects of anthropogenic and volcanic aerosols and greenhouse gases on twentieth century Sahel precipitation, Scientific Reports, 10, 12203, https://doi.org/10.1038/s41598-020-68356-w, 2020.

Hewitt, H. T., Copsey, D., Culverwell, I. D., Harris, C. M., Hill, R. S. R., Keen, A. B., McLaren, A. J., and Hunke, E. C.: Design and implementation of the infrastructure of HadGEM3: The next-generation Met Office climate modelling system, Geoscientific Model Development, 4, 223–253, https://doi.org/10.5194/gmd-4-223-2011, 2011.

Hewitt, H. T., Roberts, M., Mathiot, P., Biastoch, A., Blockley, E., Chassignet, E. P., Fox-Kemper, B., Hyder, P., Marshall, D. P., Popova, E., Treguier, A. M., Zanna, L., Yool, A., Yu, Y., Beadling, R., Bell, M., Kuhlbrodt, T., Arsouze, T., Bellucci, A., Castruccio, F., Gan, B., Putrasahan, D., Roberts, C. D., Van Roekel, L., and Zhang, Q.: Resolving and Parameterising the Ocean Mesoscale in Earth System Models, https://doi.org/10.1007/s40641-020-00164-w, 1 December 2020.

Hirasawa, H., Kushner, P. J., Sigmond, M., Fye, J., and Deser, C.: Anthropogenic aerosols dominate forced multidecadal sahel precipitation change through distinct atmospheric and oceanic drivers, Journal of Climate, 33, 10187–10204, https://doi.org/10.1175/JCLI-D-19-0829.1, 2020.

Hwang, Y. T., Frierson, D. M. W., and Kang, S. M.: Anthropogenic sulfate aerosol and the southward shift of tropical precipitation in the late 20th century, Geophysical Research Letters, 40, 2845–2850, https://doi.org/10.1002/grl.50502, 2013.

Iles, C. E., Hegerl, G. C., Schurer, A. P., and Zhang, X.: The effect of volcanic eruptions on global precipitation, Journal of Geophysical Research Atmospheres, 118, 8770–8786, https://doi.org/10.1002/jgrd.50678, 2013.

Kang, S. M.: Extratropical Influence on the Tropical Rainfall Distribution, https://doi.org/10.1007/s40641-020-00154-y, 1 March 2020.

Kang, S. M., Held, I. M., Frierson, D. M. W., and Zhao, M.: The response of the ITCZ to extratropical thermal forcing: Idealized slab-ocean experiments with a GCM, Journal of Climate, 21, 3521–3532, https://doi.org/10.1175/2007JCLI2146.1, 2008.

Kang, S. M., Frierson, D. M. W., and Held, I. M.: The Tropical Response to Extratropical Thermal Forcing in an Idealized GCM: The Importance of Radiative Feedbacks and Convective Parameterization, Journal of the Atmospheric Sciences, 66, 2812–2827, https://doi.org/10.1175/2009JAS2924.1, 2009.

Kang, S. M., Shin, Y., and Xie, S.-P.: Extratropical forcing and tropical rainfall distribution: energetics framework and ocean Ekman advection, npj Climate and Atmospheric Science, 1, 1–10, https://doi.org/10.1038/s41612-017-0004-6, 2018a.

Kang, S. M., Shin, Y., and Xie, S. P.: Extratropical forcing and tropical rainfall distribution: energetics framework and ocean Ekman advection, https://doi.org/10.1038/s41612-017-0004-6, 9 December 2018b.

Kang, S. M., Xie, S. P., Deser, C., and Xiang, B.: Zonal mean and shift modes of historical climate response to evolving aerosol distribution, Science Bulletin, 66, 2405–2411, https://doi.org/10.1016/j.scib.2021.07.013, 2021.

Lamarque, J. F., Bond, T. C., Eyring, V., Granier, C., Heil, A., Klimont, Z., Lee, D., Liousse, C., Mieville, A., Owen, B., Schultz, M. G., Shindell, D., Smith, S. J., Stehfest, E., Van Aardenne, J., Cooper, O. R., Kainuma, M., Mahowald, N., McConnell, J. R., Naik, V., Riahi, K., and Van Vuuren, D. P.: Historical (1850-2000) gridded anthropogenic and biomass

burning emissions of reactive gases and aerosols: Methodology and application, Atmospheric Chemistry and Physics, 10, 7017–7039, https://doi.org/10.5194/acp-10-7017-2010, 2010.

Lund, M. T., Myhre, G., and Samset, B. H.: Anthropogenic aerosol forcing under the Shared Socioeconomic Pathways, Atmospheric Chemistry and Physics, 19, 13827–13839, https://doi.org/10.5194/acp-2019-606, 2019.

Mamalakis, A., Randerson, J. T., Yu, J. Y., Pritchard, M. S., Magnusdottir, G., Smyth, P., Levine, P. A., Yu, S., and Foufoula-Georgiou, E.: Zonally contrasting shifts of the tropical rain belt in response to climate change, Nature Climate Change, 11, 143–151, https://doi.org/10.1038/s41558-020-00963-x, 2021.

Mann, G. W., Carslaw, K. S., Spracklen, D. V., Ridley, D. A., Manktelow, P. T., Chipperfield, M. P., Pickering, S. J., and Johnson, C. E.: Description and evaluation of GLOMAP-mode: a modal global aerosol microphysics model for the UKCA composition-climate model, Geoscientific Model Development, 3, 519–551, https://doi.org/10.5194/gmd-3-519-2010, 2010.

McFarlane, A. A. and Frierson, D. M. W.: The role of ocean fluxes and radiative forcings in determining tropical rainfall shifts in RCP8.5 simulations, Geophysical Research Letters, 44, 8656–8664, https://doi.org/10.1002/2017GL074473, 2017.

Menary, M. B., Robson, J., Allan, R. P., Booth, B. B. B., Cassou, C., Gastineau, G., Gregory, J., Hodson, D., Jones, C., Mignot, J., Ringer, M., Sutton, R., Wilcox, L., and Zhang, R.: Aerosol-Forced AMOC Changes in CMIP6 Historical Simulations, Geophysical Research Letters, 47, https://doi.org/10.1029/2020GL088166, 2020.

Moreno-Chamarro, E., Marshall, J., and Delworth, T. L.: Linking ITCZ Migrations to the AMOC and North Atlantic/Pacific SST Decadal Variability, Journal of Climate, 33, 893–905, https://doi.org/10.1175/JCLI-D-19-0258.1, 2020.

Murphy, J. M., Harris, G. R., Sexton, D. M. H., Kendon, E. J., Bett, P. E., Clark, R. T., Eagle, K. E., Fosser, G., Fung, F., Lowe, J. A., McDonald, R. E., McInnes, R. N., McSweeney, C. F., Mitchell, J. F. B., Rostron, J. W., Thornton, H. E., Tucker, S., and Yamazaki, K.: UKCP18: Land Projections Science Report, 2018.

Myhre, G., Shindell, D., Aamaas, B., Boucher, O., Dalsøren, S., Daniel, J., Forster, P., Granier, C., Haigh, J., and Hodnebrog, Ø.: Anthropogenic and natural radiative forcing, in: Climate Change 2013 the Physical Science Basis: Working Group I Contribution to the Fifth Assessment Report of the Intergovernmental Panel on Climate Change, vol. 9781107057, 659–740, https://doi.org/10.1017/CBO9781107415324.018, 2013.

Nazarenko, L., Rind, D., Tsigaridis, K., Del Genio, A. D., Kelley, M., and Tausnev, N.: Interactive nature of climate change and aerosol forcing, Journal of Geophysical Research: Atmospheres, 122, 3457–3480, https://doi.org/10.1002/2016JD025809, 2017.

Rao, S., Klimont, Z., Smith, S. J., Van Dingenen, R., Dentener, F., Bouwman, L., Riahi, K., Amann, M., Bodirsky, B. L., van Vuuren, D. P., Aleluia Reis, L., Calvin, K., Drouet, L., Fricko, O., Fujimori, S., Gernaat, D., Havlik, P., Harmsen, M., Hasegawa, T., Heyes, C., Hilaire, J., Luderer, G., Masui, T., Stehfest, E., Strefler, J., van der Sluis, S., and Tavoni, M.: Future air pollution in the Shared Socio-economic Pathways, Global Environmental Change, 42, 346–358, https://doi.org/10.1016/j.gloenvcha.2016.05.012, 2017.

Regayre, L. A., Johnson, J. S., Yoshioka, M., Pringle, K. J., Sexton, D. M. H., Booth, B. B. B., Lee, L., Bellouin, N., and Carslaw, K.: Aerosol and physical atmosphere model parameters are both important sources of uncertainty in aerosol ERF, Atmospheric Chemistry and Physics, 18, 1–54, https://doi.org/10.5194/acp-2018-175, 2018.

Riahi, K., Rao, S., Krey, V., Cho, C., Chirkov, V., Fischer, G., Kindermann, G., Nakicenovic, N., and Rafaj, P.: RCP 8.5-A scenario of comparatively high greenhouse gas emissions, Climatic Change, 109, 33–57, https://doi.org/10.1007/s10584-011-0149-y, 2011.

Rotstayn, L. D. and Lohmann, U.: Tropical Rainfall Trends and the Indirect Aerosol Effect, Journal of Climate, 15, 2103–2116, https://doi.org/10.1175/1520-0442(2002)015<2103:TRTATI>2.0.CO;2, 2002.

Rotstayn, L. D., Ryan, B. F., and Penner, J. E.: Precipitation changes in a GCM resulting from the indirect effects of anthropogenic aerosols, Geophysical Research Letters, 27, 3045–3048, https://doi.org/https://doi.org/10.1029/2000GL011737, 2000.

Rotstayn, L. D., Collier, M. A., and Luo, J.-J.: Effects of declining aerosols on projections of zonally averaged tropical precipitation, Environmental Research Letters, 10, 044018, https://doi.org/10.1088/1748-9326/10/4/044018, 2015.

Schleussner, C. F., Levermann, A., and Meinshausen, M.: Probabilistic projections of the Atlantic overturning, Climatic Change, 127, 579–586, https://doi.org/10.1007/s10584-014-1265-2, 2014.

Sexton, D., Yamazaki, K., Murphy, J., and Rostron, J.: Assessment of drifts and internal variability in UKCP projections, 2020.

Sexton, D. M. H., McSweeney, C. F., Rostron, J. W., Yamazaki, K., Booth, B. B. B., Johnson, J., Murphy, J. M., and Regayre, L.: A perturbed parameter ensemble of HadGEM3-GC3.05 coupled model projections: part 1: selecting the parameter combinations, Clim Dyn, 2021.

Smith, C. J., Kramer, R. J., Myhre, G., Alterskjær, K., Collins, W., Sima, A., Boucher, O., Dufresne, J. L., Nabat, P., Michou, M., Yukimoto, S., Cole, J., Paynter, D. J., Shiogama, H., O'Connor, F. M., Robertson, E., Wiltshire, A., Andrews, T., Hannay, C., Miller, R., Nazarenko, L., Kirkevåg, A., Olivié, D., Fiedler, S., Pincus, R., and Forster, P. M.: Effective radiative forcing and rapid adjustments in CMIP6 models, Atmospheric Chemistry and Physics Discussions, 2020.

Takemura, T.: Return to different climate states by reducing sulphate aerosols under future CO2 concentrations, Scientific Reports, 10, 21748, https://doi.org/10.1038/s41598-020-78805-1, 2020.

Taylor, K. E., Crucifix, M., Braconnot, P., Hewitt, C. D., Doutriaux, C., Broccoli, A. J., Mitchell, J. F. B., and Webb, M. J.: Estimating shortwave radiative forcing and response in climate models, Journal of Climate, 20, 2530–2543, https://doi.org/10.1175/JCLI4143.1, 2007.

Taylor, K. E., Stouffer, R. J., and Meehl, G. A.: An Overview of CMIP5 and the Experiment Design, Bull Am Meteorol Soc, 93, 485–498, https://doi.org/10.1175/BAMS-D-11-00094.1, 2012a.

Taylor, K. E., Stouffer, R. J., and Meehl, G. A.: An overview of CMIP5 and the experiment design, https://doi.org/10.1175/BAMS-D-11-00094.1, 2012b.

Thompson, D. W. J., Wallace, J. M., Kennedy, J. J., and Jones, P. D.: An abrupt drop in Northern Hemisphere sea surface temperature around 1970, Nature, 467, 444–447, https://doi.org/10.1038/nature09394, 2010.

Utida, G., Cruz, F. W., Etourneau, J., Bouloubassi, I., Schefuß, E., Vuille, M., Novello, V. F., Prado, L. F., Sifeddine, A., Klein, V., Zular, A., Viana, J. C. C., and Turcq, B.: Tropical South Atlantic influence on Northeastern Brazil precipitation and ITCZ displacement during the past 2300 years, Scientific Reports, 9, 1–8, https://doi.org/10.1038/s41598-018-38003-6, 2019.

Voigt, A., Pincus, R., Stevens, B., Bony, S., Boucher, O., Bellouin, N., Lewinschal, A., Medeiros, B., Wang, Z., and Zhang, H.: Fast and slow shifts of the zonal-mean intertropical convergence zone in response to an idealized anthropogenic aerosol, Journal of Advances in Modeling Earth Systems, 9, 870–892, https://doi.org/10.1002/2016MS000902, 2017.

van Vuuren, D. P., Stehfest, E., den Elzen, M. G. J., Kram, T., van Vliet, J., Deetman, S., Isaac, M., Goldewijk, K. K., Hof, A., Beltran, A. M., Oostenrijk, R., and van Ruijven, B.: RCP2.6: Exploring the possibility to keep global mean temperature increase below 2°C, Climatic Change, 109, 95–116, https://doi.org/10.1007/s10584-011-0152-3, 2011a.

van Vuuren, D. P., Edmonds, J., Kainuma, M., Riahi, K., Thomson, A., Hibbard, K., Hurtt, G. C., Kram, T., Krey, V., Lamarque, J.-F., Masui, T., Meinshausen, M., Nakicenovic, N., Smith, S. J., and Rose, S. K.: The representative concentration pathways: an overview, Climatic Change, 109, 5–31, https://doi.org/10.1007/s10584-011-0148-z, 2011b.

Walters, D., Baran, A. J., Boutle, I., Brooks, M., Earnshaw, P., Edwards, J., Furtado, K., Hill, P., Lock, A., Manners, J., Morcrette, C., Mulcahy, J., Sanchez, C., Smith, C., Stratton, R., Tennant, W., Tomassini, L., Van Weverberg, K., Vosper, S., Willett, M., Browse, J., Bushell, A., Carslaw, K., Dalvi, M., Essery, R., Gedney, N., Hardiman, S., Johnson, B., Johnson, C., Jones, A., Jones, C., Mann, G., Milton, S., Rumbold, H., Sellar, A., Ujiie, M., Whitall, M., Williams, K., and Zerroukat, M.: The Met Office Unified Model Global Atmosphere 7.0/7.1 and JULES Global Land 7.0 configurations, Geosci. Model Dev., 12, 1909–1963, https://doi.org/10.5194/gmd-12-1909-2019, 2019.

Williams, K. D., Jones, A., Roberts, D. L., Senior, C. A., and Woodage, M. J.: The response of the climate system to the indirect effects of anthropogenic sulfate aerosol, Climate Dynamics, 17, 845–856, https://doi.org/10.1007/s003820100150, 2001.

Williams, K. D., Copsey, D., Blockley, E. W., Bodas-Salcedo, A., Calvert, D., Comer, R., Davis, P., Graham, T., Hewitt, H. T., Hill, R., Hyder, P., Ineson, S., Johns, T. C., Keen, A. B., Lee, R. W., Megann, A., Milton, S. F., Rae, J. G. L., Roberts, M. J., Scaife, A. A., Schiemann, R., Storkey, D., Thorpe, L., Watterson, I. G., Walters, D. N., West, A., Wood, R. A., Woollings, T., and Xavier, P. K.: The Met Office Global Coupled Model 3.0 and 3.1 (GC3.0 and GC3.1) Configurations, Journal of Advances in Modeling Earth Systems, 10, 357–380, https://doi.org/10.1002/2017MS001115, 2018.

Yamazaki, K., Sexton, D. M. H., Rostron, J. W., McSweeney, C. F., Murphy, J. M., and Harris, G. R.: A perturbed parameter ensemble of HadGEM3-GC3.05 coupled model projections: part 2: global performance and future changes, Climate Dynamics, 56, 3437–3471, https://doi.org/10.1007/s00382-020-05608-5, 2021.

Zelinka, M. D., Andrews, T., Forster, P. M., and Taylor, K. E.: Quantifying components of aerosol-cloud-radiation interactions in climate models, Journal of Geophysical Research: Atmospheres, 119, 7599–7615, https://doi.org/10.1002/2014JD021710, 2014.

Zhang, S., Stier, P., and Watson-Parris, D.: On the contribution of fast and slow responses to precipitation changes caused by aerosol perturbations, Atmospheric Chemistry and Physics, 21, 10179–10197, https://doi.org/10.5194/acp-21-10179-2021, 2021.

140